Designing Flow and Temperature Uniformities in Parallel Microchannels Reactor

Ma'moun Al-Rawashdeh, Fangyuan Yue, Narendra G. Patil, T. A. Nijhuis, Volker Hessel, and Jaap C. Schouten
Dept. of Chemical Engineering and Chemistry, Laboratory of Chemical Reactor Engineering, Eindhoven University of Technology, Eindhoven 5600 MB, The Netherlands

Evgeny V. Rebrov
Reactor and Process Engineering, School of Chemistry and Chemical Engineering, Queen's University Belfast, Belfast BT9 5AG, U.K

DOI 10.1002/aic.14443
Published online March 31, 2014 in Wiley Online Library (wileyonlinelibrary.com)

A design methodology is proposed to maintain gas and liquid flow nonuniformities below an acceptable limit in a parallel micro/millichannels reactor by determining the maximum allowed temperature deviation in each part of the reactor. The effect of temperature deviation on flow distribution was quantified using a hydraulic resistive network model. The effect of flow rate on temperature deviation was demonstrated using a one-dimensional energy balance model. Experiments were conducted using the barrier-based micro/millichannels reactor (BMMR). Flow distribution in the BMMR is based on placing hydraulic resistances (barrier channels) in the gas and liquid manifolds to regulate the flows. Temperature deviation in the barrier channels affects flow nonuniformity by 10 times more than in the reaction channels. Above a certain critical liquid residence time, flow rate has no significant effect on the temperature deviation which depends on the liquid used, reactor material of construction, and its geometrical dimensions. © 2014 American Institute of Chemical Engineers *AIChE J*, 60: 1941–1952, 2014
Keywords: design, multiphase flow, heat transfer, mathematical modeling, microreactors

Introduction

Microstructured reactors are viable reactors for highly exothermic and mass-transfer limited reactions. This makes them attractive devices to improve safety, reduce waste, and enhance product selectivity, as well as conversion.[1–5] For a single microchannel reactor, the flow rate is often in the range of mL/min which is suited for a g/h production rate. Scale-up is required to reach kg/h and ton/h production rates. Scale-up route in microchannel reactors can be achieved in three consecutive steps.[6] First, the microchannel cross-sectional dimensions are scaled-up while maintaining the mass- and heat-transfer properties of the single microchannel.[7,8] Second, numbering-up is achieved by placing multiple channels in parallel in one modular unit. The third step is made by placing multiple modular units in parallel.

For heterogeneously catalyzed gas-phase reactions in microreactors, scale-up and numbering up to thousands of parallel channels was successfully demonstrated.[9,10] Also, for liquid-phase reactions, scale-up was successfully demonstrated, but only for a limited number of parallel channels due to the complexity of flow distribution.[11–13] For gas-liquid processing and using the concept of numbering-up, the throughput is still mostly restricted at the laboratory scale at g/h due to the complexity and expenditure needed for an adequate numbering-up with a uniform flow distribution.[14–18]

It is difficult to achieve exact uniform flow distribution in numbered-up microchannel reactors. Usually an acceptable target for flow nonuniformity is defined according to the process and the required quality of the product. The design principle for most flow distributors relies on controlling the hydraulic flow resistances in the device. This is described by the pressure drop in each of the parallel channels. In microfluidic devices, the resistive network RN model is often used to predict the influence of these resistances.[19,20] The RN model is, however, only valid for very low Reynolds number in the laminar flow range, which is the case for most of the microfluidic devices. The pressure drop in a microchannel is the product of the hydraulic resistance (R) and the flow rate (q) as given in Eq. 1

$$\Delta P = Rq \tag{1}$$

For single-phase flow, the Hagen–Poiseuille equation can be used to estimate the pressure drop for a given flow rate q.[20] In that case, the hydraulic resistance R is as given in Eq. 2

$$R = \frac{32\mu L\lambda_{NC}}{d^2 A} \tag{2}$$

where μ is the viscosity, L is the channel length, λ_{NC} is the noncircularity factor that depends on the channel geometry, A

Correspondence concerning this article should be addressed to J. C. Schouten at j.c.Schouten@tue.nl.

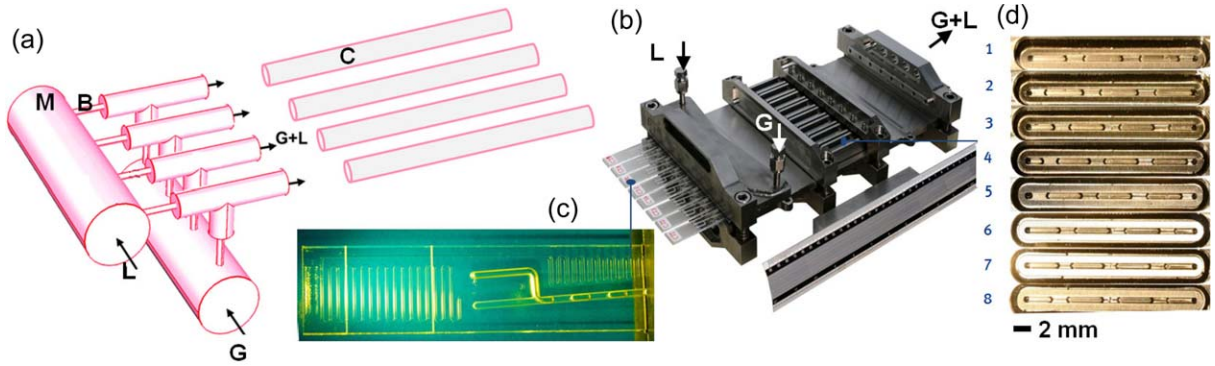

Figure 1. (a) A schematic view of the BMMR with four parallel microchannels; symbols used are G gas, L liquid, M manifold, B barrier channel, C gas-liquid microchannel; (b) picture of the BMMR which consists of eight parallel microchannels; (c) an enlarged view of the glass picture which has the gas and liquid barrier channels and the T mixer; (d) a picture of Taylor flow in the eight parallel microchannels.

[Color figure can be viewed in the online issue, which is available at wileyonlinelibrary.com.]

is the channel cross section area, and d is the hydraulic diameter.[19] The hydraulic resistance is a function of the channel hydraulic diameter to the power four. Therefore, channel diameter has a significant influence on flow distribution. The second parameter which influences the hydraulic resistance is the viscosity which changes with the fluid composition and temperature. A few studies have been made to investigate the effect of flow and temperature distribution in microreactors.[8,21,22] This is because many phenomena play a role in such a study: flow hydrodynamics, heat exchanger design, and reaction kinetics. Quantifying the interplay between these phenomena requires advanced analytical techniques such as computational fluid dynamics (CFD). Additionally, modeling of multiphase flow in parallel microchannels increases the complexity of the CFD modeling dramatically. Having an alternative and a more simple technique to study the effect of flow and temperature distribution is, therefore, a valuable asset for microreactor designs specially for microreactor applications which involve multiphase flow.

The barrier-based micro/millichannels reactor (BMMR) is a structured multiphase microreactor which reaches large scale production via numbering-up.[23–25] Uniform flow distribution is achieved in the BMMR by placing hydraulic resistances, so called barrier channels (B), between the parallel microchannels (C) and the separate gas and liquid feeding manifolds (M) as shown in Figure 1. This approach has the following advantages: (1) gas-liquid channeling is prevented, (2) all flow regimes, viz. Taylor, churn, and annular can be successfully realized, and (3) the flow uniformity is substantially improved.

The hydraulic resistances of the barrier channels can be quantified in a generic way as $\Delta\tilde{P}_B$ as given in Eq. 3. It is the average pressure drop over the barrier channels, $\overline{\Delta P_B}$, divided by the average pressure drop over the corresponding mixers and microchannels, $\overline{\Delta P_C}$. Since $\Delta\tilde{P}_B$ is a ratio of pressure drops, it is dimensionless

$$\Delta\tilde{P}_B = \frac{\overline{\Delta P_B}}{\overline{\Delta P_C}} \tag{3}$$

Early studies in the field have demonstrated this type of distributor in microchannel reactors.[23,24] Their designs were successfully run with barrier channels dimensions giving $\Delta\tilde{P}_B$ larger than 25 and 50 for liquid and gas, respectively. In Al-Rawashdeh et al.,[26] we have demonstrated that $\Delta\tilde{P}_B$ can be designed in the range of 4–25 by following a specific design methodology. Cut-off values of the maximum acceptable fabrication tolerance in the barrier channels, mixers and reaction channels diameters were determined using the proposed design methodology.

The aim of this article is to study the effect of temperature and flow distribution for gas-liquid Taylor flow in the BMMR. A simpler approach is proposed compared to that of a CFD. First, a predefined temperature deviation in the parallel microchannels is applied. Then, the RN model is used to estimate the influence of temperature on the flow distribution. Second, one-dimensional energy balance model is used to study the influence of flow on the temperature deviation. The models are validated experimentally using the BMMR. Using these results, a design methodology is proposed to determine the maximum allowed temperature deviation in the parallel microchannels to keep flow nonuniformity below an acceptable limit.

Modeling and Methodology

Temperature nonuniformity

In microchannels reactor, there are several possible temperature nonuniformities. For sake of simplification, temperature nonuniformities are represented by three temperature deviation factors as will be explained next. These factors will be used to study the effect of temperature on flow distribution.

The BMMR is divided into three parts: manifold M, barrier channels B, and mixer and reaction channels C represented by three colors as shown in Figure 2a. One average temperature T_{avg} is used in each part and per parallel microchannel as shown in Figure 2b. As a result, a number of N different average temperatures is obtained for each of the BMMR parts. Quantifying the difference between these average temperatures gives the three temperature deviation factors as $\sigma(T_M)$, $\sigma(T_B)$, and $\sigma(T_C)$ for manifold, barrier, and reaction channels, respectively. $\sigma(T)$ is obtained according to Eq. 4, where $T_{avg,i}$ is the average temperature for microchannel number i for any of the BMMR parts: M, B, or C; $\bar{T}_{avg}$ is the average temperature for any of the parts, M, B, or C, over the entire number of parallel microchannels N.

$$\sigma(T) = \sqrt{\frac{\Sigma_i (T_{avg,i} - \bar{T}_{avg})^2}{N-1}} \tag{4}$$

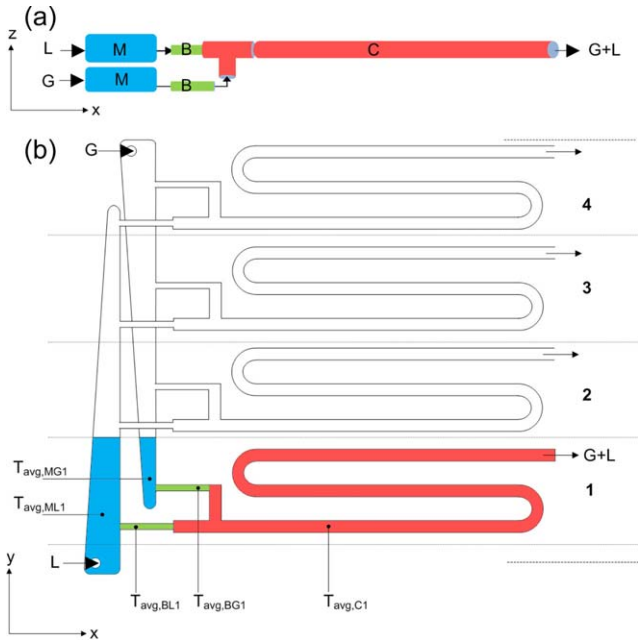

Figure 2. (a): Schematic cross-sectional view of a single channel BMMR showing the manifolds M, barrier channels B, mixer and reaction channel C, gas G and liquid L; (b) schematic top cross view of BMMR for four parallel microchannels. Average temperature for M, B, and C are shown in three different colors for microchannel number one.

[Color figure can be viewed in the online issue, which is available at wileyonlinelibrary.com.]

Resistive network model

The RN model was extended to account for multiphase flow which was called the 2-phase resistive network (2-PRN) model.[26] The 2-PRN model was developed for gas-liquid Taylor flow and was experimentally verified. For a given temperature deviation, the 2-PRN model can be used to evaluate the effect of temperature on flow distribution. However, the 2-PRN model has some limitations. First, it is valid only at low Reynolds number. Second, the 2-PRN model cannot evaluate the effect of flow on temperature deviation. Third, only one value for the temperature can be used for each hydraulic resistance independent of the axial length and cross-sectional temperature profiles. Due to these limitations, an energy balance was developed to study the effect of flow rate on temperature deviation in the BMMR.

Energy balance model

The effect of flow rate on the temperature deviation was accounted for by using a one-dimensional energy balance model as shown in Figure 3. The energy balance was applied for a single microchannel C through which gas-liquid Taylor flow was passing without any reaction. A uniform heat supply Q_{supply} was applied to the single microchannel C while no heat was supplied to the other parts of the BMMR. Heat exchange between the gas-liquid microchannel C and the other parts of the BMMR was taken into account via heat conduction as will be explained later. By changing the flow rate, temperature profiles were generated which allowed studying the effect of flow rate on temperature deviation.

Few assumptions were made to construct the energy balance model: constant physical properties; plug flow for both gas and liquid, negligible axial dispersion; no reaction in the gas-liquid Taylor flow; heat supply to the reaction channel is applied only at a fixed reference temperature along the axial direction; fixed heat loss to the surroundings and heat conduction to the other BMMR parts.

The first energy balance was made for the gas-liquid phase in the microchannel and it consisted of three terms as shown in Figure 3 and in Eq. 5. The three energy terms used to generate the temperature profile in the microchannel were the convective inlet and outlet heat transport (Q_{in} and Q_{out}) and heat exchange at the channel wall (Q_{exch}). Usually the heat taken by the gas phase was less than 1% compared to that taken by the liquid phase. Therefore, energy balance over the gas phase was neglected. However, the influence of the gas flow rate was still included when computing the gas-liquid heat-transfer coefficient

$$Q_{out} - Q_{in} = Q_{exch} \tag{5}$$

$$mc_p \frac{dT}{dx} = h_{wc} A_c (T_w - T) \tag{6}$$

The energy balance was made for the liquid phase in the microchannel as shown in Eq. 6, where m is the mass flow rate, C_p is the heat capacity of the liquid, h_{wc} is the overall gas-liquid-solid heat-transfer coefficient (W m^{-2} K^{-1}), and A_i is the heat exchanger surface area (m^2). The overall gas-liquid-solid heat-transfer coefficient was estimated using the heat resistance in series model as shown in Eq. 7. It consisted of the heat-transfer resistance in the channel walls ($\frac{d_w}{k_w}$) and the heat-transfer resistance in the gas-liquid flow ($\frac{1}{h_{GL}}$)

$$\frac{1}{h_{wc}} = \frac{1}{h_{GL}} + \frac{d_w}{k_w} \tag{7}$$

To calculate the heat-transfer coefficient h_{GL}, the entrance effects were neglected and a correlation for the Nusselt number for gas-liquid Taylor flow was taken from literature[27] as shown in Eqs. 8 and 9

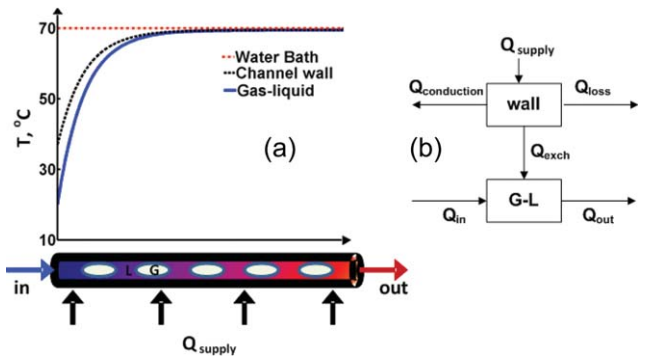

Figure 3. (a) Axial temperature profiles for gas-liquid Taylor flow, microchannel wall, and for the water heating bath; (b) a drawing of the terms in the energy balance for the gas-liquid microchannel (G-L) and the microchannel wall which are given in Eq. 5 and in Eq. 10, respectively.

[Color figure can be viewed in the online issue, which is available at wileyonlinelibrary.com.]

$$Nu = \frac{L_s}{L_s + L_B}\left(4.364 + \frac{a_1}{L_s^* + a_2 L_s^{*1/3}}\right) \quad (8)$$

$$L_s^* = \frac{L_s}{Re_{GL}\, Prd} \quad (9)$$

where $a_1 = 0.29$, $a_2 = 0.15$, and $Nu = \frac{h_{GL}d}{k}$ is the Nusselt number for gas-liquid Taylor flow, d is the channel diameter (m), k is the thermal conductivity of liquid (W/m.K), L_s and L_b are the slug and bubble lengths (m), Re_{GL} is gas-liquid Reynolds number $Re_{GL} = \frac{d\rho u_{GL}}{\mu}$ and Pr is the Prandtl number $Pr = \frac{C_p \mu}{k}$.

Note that Eq. 6 assuming a negligible temperature profile in the cross-sectional plane of the microchannel wall. This assumption is only correct if the Biot number Bi is much lower than 1. Here the Bi is between 0.2 and 0.4. The assumption therefore results in a small error. However, the resulted error will have a negligible influence on the outcome of this study because: (1) a steady-state situation is maintained in this study with a uniform heat supply along the axial length; (2) the error is in all of the parallel microchannels; (3) the aim of the study is the relative difference in the temperatures in the parallel channels rather than the absolute temperatures. Therefore and for sake of simplicity, a lumped treatment for the energy balance is maintained.

The second energy balance was made over the microchannel wall. The energy balance consisted of four terms as shown in Figure 3 and in Eq. 10: heat transfer from the hot fluid to the channel wall, Q_{supply}, heat transfer from the channel wall to the gas-liquid Taylor flow, Q_{exch}, heat loss by conduction to the adjacent devices (manifolds and barrier channels), $Q_{conduction}$, and heat loss by convection to the surroundings, Q_{loss}. Axial heat dispersion was neglected because uniform heat supply at a fixed temperature was maintained. The energy balance over the microchannel wall was written as given in Eq. 11. Explanations about the used heat-transfer coefficients are given next

$$Q_{supply} - Q_{exch} - Q_{conduction} - Q_{loss} = 0 \quad (10)$$

$$h_{mc}A_{supp}(T_h - T_w) - h_{wc}A_c(T_w - T) - h_{cond}A_{cond}(T_w - T_{joint}) - h_{loss}A_{loss}(T_w - T_{surr}) = 0 \quad (11)$$

h_{mc} is the heat-transfer coefficient for the heat transfer from the heating source to the microchannel wall. h_{mc} depends on the type of the heat exchanger. In the experimental setup, heat was supplied by putting the gas-liquid microchannel in a water heating bath. Thus, h_{mc} was assumed as heat-transfer coefficient on a free surface, a value of 500 W/m^2.K was used.[28] h_{cond} is the heat-transfer coefficient for the heat transfer between the gas-liquid microchannel and the BMMR assembly (inlet tubes, manifolds, barrier channels, and collectors) which depends on the conductivity of the channel walls and characteristic transfer length. h_{cond} was estimated by dividing the conductivity of the microchannel wall material by the length of gas-liquid microchannel. h_{loss} is the heat-transfer coefficient for external heat losses which depends on the external surface of the device without insulation. A value equals to 5 W/m^2 K was assumed.

Equation 7 was solved simultaneously with Eq. 11 to generate axial temperature profiles for the liquid and the microchannel wall depending on the used flow rates. The channel dimensions, geometry, material of construction, and flow rates are given in the experimental section.

Design methodology

A design methodology was developed for estimating the maximum allowed variation in the channel diameter and required barrier channel dimensions to stay below a target flow nonuniformity.[26] The same design methodology was used here to quantify the effect of temperature on flow distribution. The working principle of the methodology is to decouple the effect of temperature deviation of each part of the BMMR, manifolds M, barrier channels B, and mixers and reaction channels C, alone and then combine their contribution to cumulative flow nonuniformity. Full details about the methodology is given in Al-Rawashdeh et al.[26]

A temperature deviation, quantified by Eq. 4, was applied to one particular part of the BMMR, M, B, or C, while the temperature of the other parts maintained at a constant and fixed temperature. Hydraulic resistances were calculated and the 2-PRN model was used to compute the flow distribution. Next, the flow rate $q_{i,after}$ of each microchannel was normalized according to Eq. 12 by its respective flow rate $q_{i,before}$ before applying the temperature deviation. By using Eq. 13, the flow nonuniformity factor of that particular BMMR part was then calculated; where $\bar{\tilde{q}}$ is the average flow rate of the normalized flow rate and N is the number of channels. The cumulative contribution of the three flow nonuniformity factors gave the overall gas or liquid flow nonuniformity as shown in Eq. 14. $\sigma(\tilde{q})$ is the target gas or liquid flow nonuniformity quantified according to Eq. 13. The three flow nonuniformity factors are: (1) $\sigma(\tilde{q}_{T,M})$ for the effect of temperature deviation in the manifold part, $\sigma(T_M)$, (2) $\sigma(\tilde{q}_{T,B})$ for the effect of temperature deviation in the barrier channels part, $\sigma(T_B)$, and (3) $\sigma(\tilde{q}_C)$ for the effect of temperature deviation in the mixer and reaction channels part, $\sigma(T_C)$

$$\tilde{q}_i = \frac{q_{i,after}}{q_{i,before}} \quad (12)$$

$$\sigma(\tilde{q}) = \frac{1}{\bar{\tilde{q}}}\sqrt{\frac{\Sigma_i(\tilde{q}_i - \bar{\tilde{q}})^2}{N-1}}\,100\% \quad (13)$$

$$\sigma(\tilde{q}) = \sqrt{\sigma^2(\tilde{q}_{T,M}) + \sigma^2(\tilde{q}_{T,B}) + \sigma^2(\tilde{q}_{T,C})} \quad (14)$$

Experimental Section

The experiments were conducted using in the BMMR shown in Figure1. The reaction channels are square fabricated in a stainless steel plate. Key dimensions of the BMMR are given in Table 1. Design and fabrication details of the BMMR can be found in Al-Rawashdeh et al.[6]

Table 1. Dimensions for the Barrier-Based Micro/Milli Reactor BMMR

	W, (mm)	H, (mm)	L, (mm)
Inlet gas manifold	41*	5	155
Inlet liquid manifold	41*	5	155
Gas barrier channel	0.4	0.1	340
Liquid barrier channel	1.0	0.1	37
Inlet gas T-mixer	1.3	1.3	13
Inlet liquid mixer	1.3	1.3	10
Reaction channel	1.23	1.23	2000

*The width is decreasing by an 8 degree angle. The thickness of the microchannel wall is 2 mm.

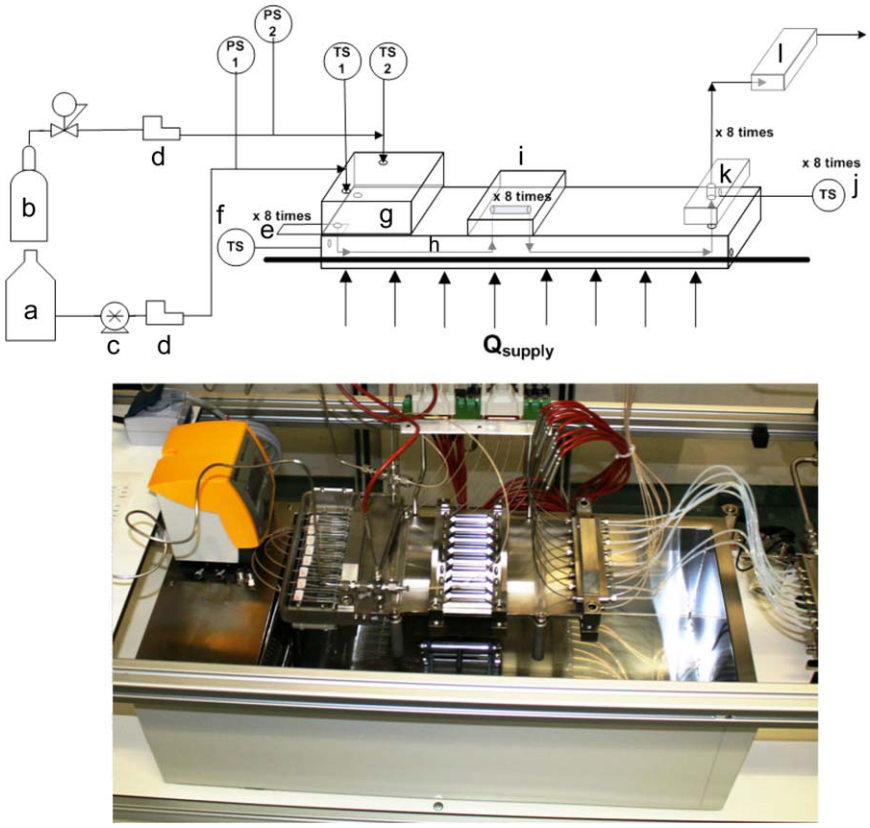

Figure 4. Process flow diagram of the experimental setup and the locations of the temperature and pressure sensors.

Symbol used: (a) liquid tank, (b) gas bottle, (c) gear pump, (d) mass flow controller, (e) BT glass chip, (f) temperature sensors at inlet, (g) manifold, (h) reaction channel plate, (i) inspection window, (j) temperature sensors at outlet, (k) connection block, and (l) collector block. The thick line represents the level in which the reactor was immersed in the water bath. Bottom: A picture of the BMMR on top of the water bath. [Color figure can be viewed in the online issue, which is available at wileyonlinelibrary.com.]

The experiments were performed using water and nitrogen at different flow rates. The liquid flow rate was changed in the range of 10–115 mL/min and the gas flow rate from 10 to 230 mLn/min. A process flow diagram of the experimental setup is shown in Figure 4. Liquid was pumped using a gear pump (NHK Mikrosysteme GmbH, MZR-7205) via a liquid mass flow controller (Bronkhorst). Nitrogen was fed from a gas bottle in a controller manner by using a mass flow controller (Bronkhorst). The pressure was measured at the manifold using a pressure sensor (range 0–25 bar, Endress+Hauser, PMP131) and temperature was measured using a thermocouple type pt100.

Heat was supplied by placing the reaction channels in a water heating bath as shown in Figure 4. The other parts of the reactor assembly were outside the water heating bath. The vapors from the water heating bath obscured the vision. Thus, it was not possible to measure slug and bubble lengths and bubble generation frequency. Instead, the flow distribution in the liquid phase was measured using the weight method. The tubes between the reactor and the collector (l) were disconnected. The liquid from each channel flowed into a separate vessel. The collected liquid volume in each vessel was weighed after reaching the steady-state condition. Flow nonuniformity was calculated using Eq. 13. The flow distribution was determined at two water bath temperatures, 20°C and at 70°C. Measuring flow distribution at higher temperatures was not possible due to the high vapor pressure because water had to be collected in an open vessel. Over the entire tested flow range, temperature nonuniformity at the outlet of the eight microchannels was measured.

Results

Effect of temperature on the pressure drop ratio, $\Delta\tilde{P}_B$

Any changes to the viscosity will affect the pressure drop which is the key parameter to flow distribution. Viscosity changes as a function of temperature in a different way depending on the fluid used. For demonstration, the effect of temperature on nitrogen and water viscosities is shown in Figure 5a.[29,30] Increasing the temperature decreases the water viscosity and increases the nitrogen viscosity. If this increase in temperature is implemented in a barrier-based flow distributor, the pressure drop ratio $\Delta\tilde{P}_B$ at the gas side will become larger compared to the liquid side. If the difference between $\Delta\tilde{P}_B$ of the gas and liquid sides is too large, gas-liquid channeling is expected.[25] Therefore, when designing a barrier-based flow distributor the range of operating temperature in the barrier channels should be specified.

Effect of temperature on flow distribution

The Manifold Flow Nonuniformity Factor, $\sigma(\tilde{q}_{T,M})$. Temperature deviation in the manifold has a negligible effect on flow distribution. The manifolds hydraulic resistances, $R_{M,i}$, are the smallest if compared to other hydraulic resistances in the BMMR. The manifolds hydraulic resistances, $R_{M,i}$, were made the smallest by increasing the manifolds cross-

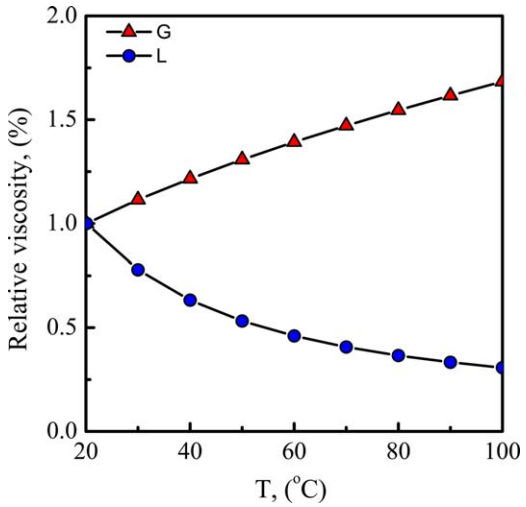

Figure 5. Theoretical effect of temperature on nitrogen and water viscosities.[29,30]

[Color figure can be viewed in the online issue, which is available at wileyonlinelibrary.com.]

sectional dimensions to an acceptable limit using the 2-PRN model. This is made on purpose to reduce the influence of manifold on the flow distribution. The effect of temperature deviation in the manifold part only on flow distribution is, therefore, neglected.

The Barrier Flow Nonuniformity Factor, $\sigma(\tilde{q}_{T,B})$. The effect of temperature deviation in the barrier channels on flow distribution is shown in Figure 6. Different barrier channel dimensions were used in this study by reducing the barrier channel depth. Temperature deviation in the barrier channels has a significant influence on flow distribution. The influence is linear with a slope larger than one. For example, for a temperature deviation $\sigma(T_B)$ of 4°C, flow nonuniformity reaches 16%. As temperature deviation increases, the flow distribution slightly depends on the used pressure drop ratio $\Delta\tilde{P}_B$.

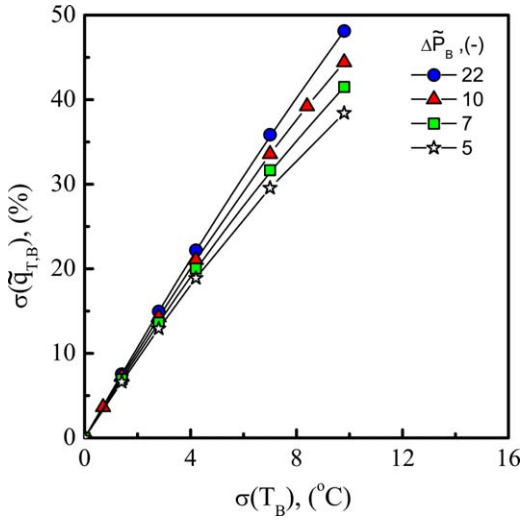

Figure 6. Effect of temperature deviation in the barrier channels on flow distribution.

Study is made at different hydraulic resistance in barrier channels $\Delta\tilde{P}_B$ and at an average temperature of 20°C. [Color figure can be viewed in the online issue, which is available at wileyonlinelibrary.com.]

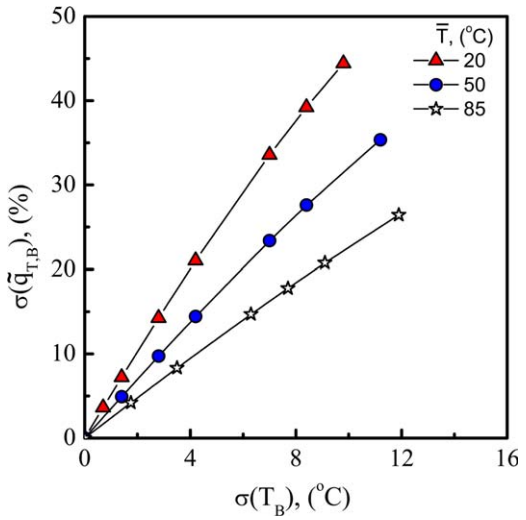

Figure 7. Effect of temperature deviation in the barrier channels on flow distribution.

Study is conducted at different average temperature of 20°C, 50°C, and 85°C all with a fixed $\Delta\tilde{P}_B$ of 10. [Color figure can be viewed in the online issue, which is available at wileyonlinelibrary.com.]

When the study in Figure 6 is repeated but at higher average temperature of 50 and 85°C, the temperature deviation in the barrier channels has a milder influence on flow distribution as shown in Figure 7. This is due to the nonlinear relation between liquid viscosity and temperature as shown in Figure 5. The relation between temperature deviation in the barrier channel and flow distribution can be represented in Eq. 15, where $f_1(T_{\text{designed}}, \mu_L)$ is a constant that depends on the designed temperature and liquid viscosity

$$\sigma(\tilde{q}_{T,B}) = f_1(T_{\text{designed}}, \mu_L)\sigma(T_B) \tag{15}$$

The Mixer and Reaction Channel Flow Nonuniformity Factor, $\sigma(\tilde{q}_C)$. The effect of temperature deviation in the mixer and reaction channels is shown in Figure 8. As

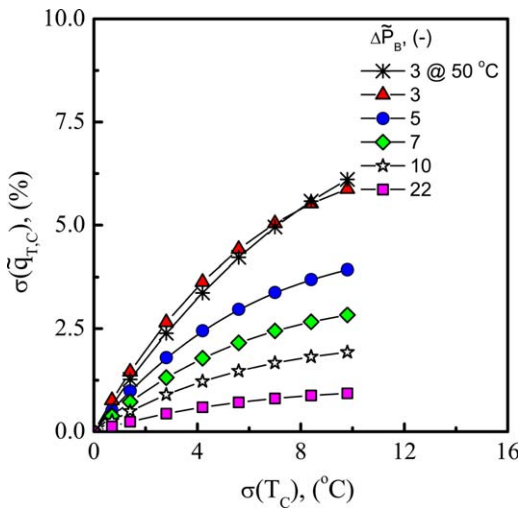

Figure 8. Effect of temperature deviation in the mixer and reaction channels on flow distribution.

Study is made at different hydraulic resistance in the barrier channels. [Color figure can be viewed in the online issue, which is available at wileyonlinelibrary.com.]

temperature deviation increases, flow nonuniformity increases depending on the pressure drop ratio, $\Delta\tilde{P}_B$. The effect of temperature deviation on flow nonuniformity reduces at larger $\Delta\tilde{P}_B$. Temperature deviation effect on flow distribution depends slightly on the operating temperature as shown when changing the average temperature from 20 to 50°C. For the entire tested range of temperature deviation, the flow nonuniformity remains less than 10%. If this compared to the barrier channels part at similar temperature deviations, the barrier channels affect flow distribution by 10 times more than in the mixer and reaction channels.

$$\sigma(\tilde{q}_C)=\frac{\sigma(\Delta P_C)}{\Delta\tilde{P}_B} \tag{16}$$

In a previous study, Eq. 16 was found to describe accurately the variational effects due to channel diameter in the mixer and reaction channels on flow distribution.[26] Here, Eq. 16 was also found to describe accurately the effect of temperature deviation in the mixer and reaction channels on flow distribution. This equation was derived based on analysis made using the 2-PRN model. It is a generic equation because it is given in term of pressure drops, the key parameter in flow distribution. All possible variations which affect pressure drop in the mixer and reaction channels are included in this equation such as: diameter, temperature, slug and bubble lengths, and flow rates.

Physical interpretation for the effect of temperature deviations on flow nonuniformity

In the last three subsections, the outcome from the 2-PRN model analysis was presented. Here, a physical interpretation on the found results is given. A dimensionless analysis for two channels in parallel is derived using the single-phase hydraulic resistance network model. Using Eq. 1 and assuming that the overall pressure drop is constant, the flow rate q depends just on the overall equivalent hydraulic resistance R_{eq}, shown as $q=\frac{\Delta P}{R_{eq}}$. The flow rate q depends linearly on $\frac{1}{R_{eq}}$. The equivalent resistance R_{eq} for two channels in parallel are derived, as shown in Eq. 17

$$\frac{1}{R_{eq}}=\frac{(R_B+R_C)_1+((R_B+R_C)_2+(R_M)_2)}{(R_B+R_C)_1((R_B+R_C)_2+(R_M)_2)} \tag{17}$$

The hydraulic resistance in the manifold R_M is much smaller compared to that in the barrier channels and mixer and reaction channels. Thus, it can be safely neglected as was done in the previous section. When the hydraulic resistance in the barrier channels R_B is much larger than R_C, then the equivalent resistance will be equal to $\frac{1}{R_{eq}}=\frac{2}{R_B}$. Thus, the flow nonuniformity will be controlled mainly by the hydraulic resistance in the barrier channels R_B. Note that the number two here refers to the number of parallel channels. As single-phase flow passes through the barrier channels, R_B can be described as given in Eq. 2, which has an inverse relation with viscosity. Therefore, the flow rate q depends linearly with viscosity as 2 μ, which is a function of the fluid compositions and the temperature. Temperature deviations in the parallel channels result in varied viscosities which consecutively result in a nonuniform flow distribution. As the barrier channels are the most important factor that affect the flow distribution in the barrier-based flow distributor, that is why temperature deviation in the barrier channel is the most significant. In this case, it is 10 times more significant than the temperature deviation in the mixer and reaction channels. However, this quantified value will vary depending on the relation between viscosity and temperature. If another fluid is used which has a different relation between viscosity and temperature, then the relation between temperature deviation and flow nonuniformity will also change.

Numerical validation of the design methodology: Effect of all combined contributions on flow distribution

In this section, the combined contribution from all flow nonuniformity factors will be demonstrated. The gas or liquid flow nonuniformity can be obtained as a cumulative contribution of all flow nonuniformity factors as given in Eq. 18. In this study, the effect of temperature deviation in the barrier via $\sigma(\tilde{q}_{T,B})$ and in the mixer and reaction channels via $\sigma(\tilde{q}_{T,C})$ will be accounted for, while the effect of temperature deviation in the manifold $\sigma(\tilde{q}_{T,M})$ will be neglected. In addition to these two factors, three other flow nonuniformity factors are included in Eq. 18. These are the flow nonuniformity factors due to variations in channel diameters which always exist in the BMMR as demonstrated in Al-Rawashdeh et al.[6] These three flow nonuniformity factors are: (1) The flow nonuniformity factor due to the manifold type and dimensions, $\sigma(\tilde{q}_M)$; (2) The flow nonuniformity factor due to the variation in the diameter of the barrier channels, $\sigma(\tilde{q}_B)$; and (3) the flow nonuniformity factor due to the variation in the internal diameter of the mixer and the reaction channels, $\sigma(\tilde{q}_C)$

$$\sigma(\tilde{q})=\sqrt{\sigma^2(\tilde{q}_M)+\sigma^2(\tilde{q}_B)+\sigma^2(\tilde{q}_C)+\sigma^2(\tilde{q}_{T,B})+\sigma^2(\tilde{q}_{T,C})} \tag{18}$$

The target from Eq. 18 is that the cumulative contribution of all flow nonuniformity factors should give an overall flow nonuniformity below an acceptable limit. For demonstration, a maximum acceptable overall flow nonuniformity of 10% was used here. To achieve this target, first a weight was given to each flow nonuniformity factor in Eq. 18 to assure that the target overall flow nonuniformity remained below 10%. Then, the assigned weight to each flow nonuniformity factor was used as a target from which the maximum allowed variation in diameter and temperature was calculated. For any of the individual flow nonuniformity factors, there was no exact weight which can be assigned. Therefore, there were different design options which can be generated. For example, Table 3 shows three different design options generated to give cut-off values of the maximum allowed variation in diameters and temperatures of the BMMR to maintain flow nonuniformity below 10%. These three design options were given here for demonstration while other design options were possible to generate. Such a variety of the design options gives the designer and the fabrication company extra room and flexibility to find the most realistic and optimal design dimensions.

Analytical validation for one of the design options is given next using the 2-PRN model. For demonstration, option 1 in Table 3 was inserted in the 2-PRN model. The model was then used to compute the overall flow nonuniformity which compared to the target value of 10%. The variations in

Table 2. Values used for Heat Transfer Experiments

ρ, kg/m^3	μ, $Pa.s$	c_p, J/$kg.K$	k, $W/m.K$	k_w, $W/m.K$
1000	0.001	4181.3	0.57	16

Density ρ, Viscosity μ, Heat capacity c_p, water thermal conductivity k, steel thermal conductivity k_w.

Table 3. Cut-off Values of the Maximum Allowed Variation in Diameters and Temperatures in the BMMR to Maintain Flow Non-uniformity Below 10%

Variable*	Option 1	Option 2	Option 3
$\sigma(d_B)$ (%)	2	1	2.3
$\sigma(d_{Mixer})$ (%)	10	15	5
$\sigma(d_C)$ (%)	15	25	10
$\sigma(T_B)$ (°C)	1	0.5	1.5
$\sigma(T_C)$ (°C)	5	12	8

*Manifold flow non-uniformity factor was assumed less than 1%. Average temperature is 20 °C.

diameter and deviations in temperature are shown in Figures 9c and 9d, respectively. The lines represent average values of these variations. The simulation was run and repeated 10,000 times. In each iteration, random values for diameter and temperature were chosen as explained in Al-Rawashdeh et al.,[26] with a maximum variation less than the cut-off values specified in Table 3. For both gas and liquid, more than 95% of the iterations gave an over all flow nonuniformity less than 10% as shown in Figure 9a. The remaining 5% of the iterations slightly deviated from the target but the maximum obtained overall flow nonuniformity did not exceed 15%. The average pressure drop ratio $\Delta\tilde{P}_B$ of both gas and liquid remained around a value of 6 as is shown in Figure 9b.

Effect of flow on temperature deviation

The one-dimensional energy balance was used to study the effect of flow on temperature deviation. A good way to plot the obtained results is shown in Figure 10. The ratio of temperature deviation to flow nonuniformity $\frac{\sigma(T)}{\sigma(q)}$ varies as a function of the liquid residence time. This ratio is described in Eq. 19 where τ_L is the liquid residence time and f_2 and f_3 are constants which depend on the liquid used, the material of construction of the BMMR and its geometrical dimensions

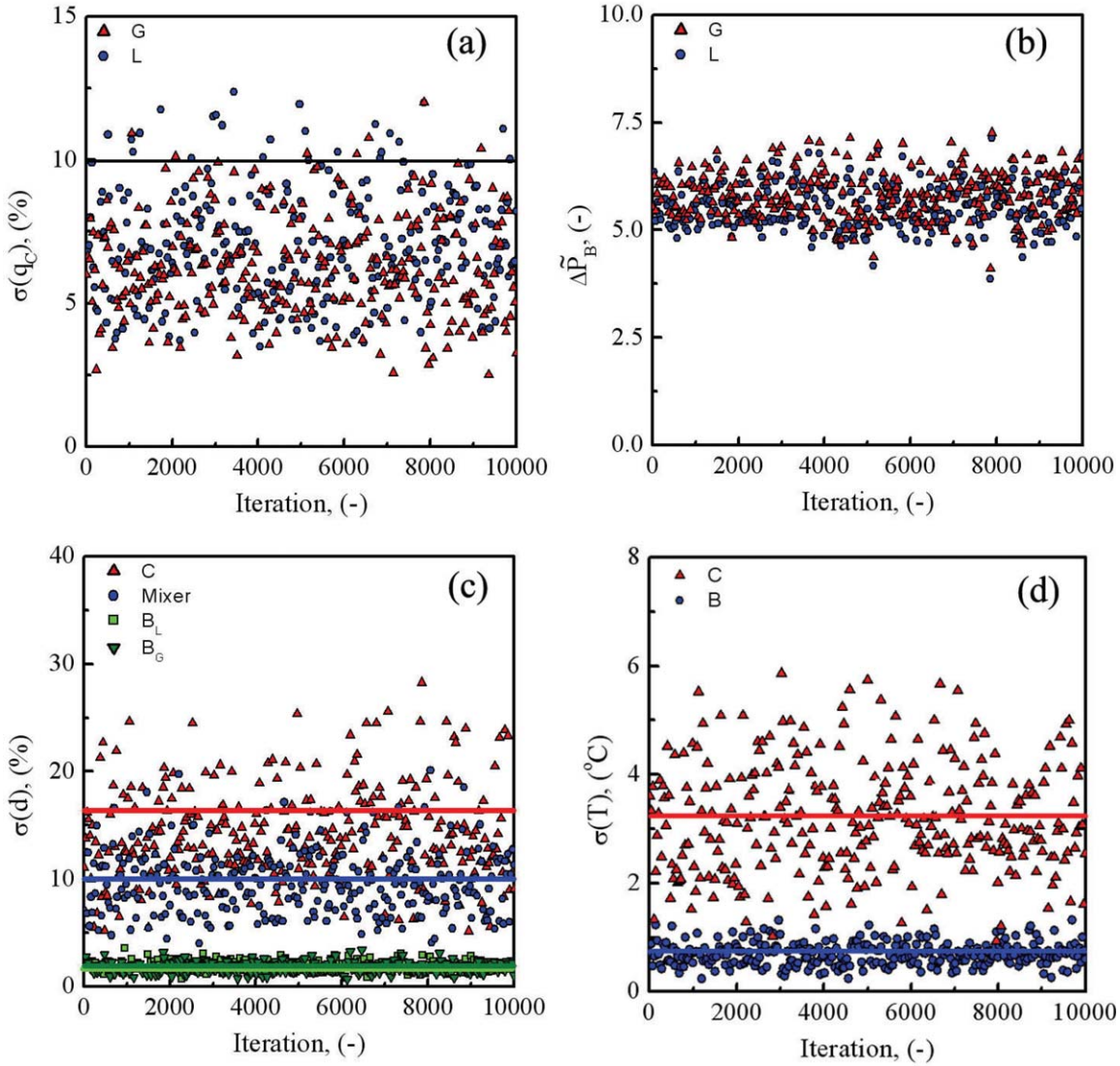

Figure 9. Effect of 10,000 random variations in channel diameter and temperature on (a) gas and liquid flow nonuniformity, (b) pressure drop ratio in barrier channels, (c) variations in diameter in different part of the reactor, and (d) deviations in temperature in barrier and reaction channels.

[Color figure can be viewed in the online issue, which is available at wileyonlinelibrary.com.]

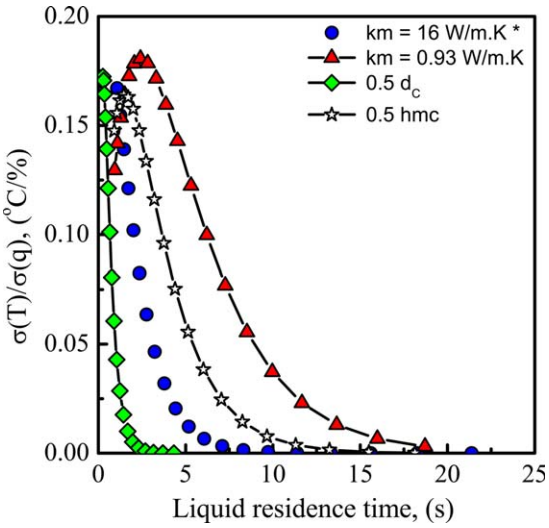

Figure 10. Effect of liquid residence time on ratio of temperature deviation to flow nonuniformity.

Study is made based on the one-dimensional energy balance. * Reference case for steel plate given in Table 2. k_m equals to 0.93 W/m.K refers to glass; 0.5 d_C is when channel diameter reduced by half; 0.5 h_{mc} is when the heat-transfer coefficient from water bath to microchannels wall reduced by half. [Color figure can be viewed in the online issue, which is available at wileyonlinelibrary.com.]

$$\frac{\sigma(T)}{\sigma(q)} = f_2 \exp\left(-f_3\, \tau_L\right) \tag{19}$$

Above a certain liquid residence time, $\frac{\sigma(T)}{\sigma(q)}$ decreases approaching almost zero. Beyond that critical liquid residence time, there is no significant effect of flow on temperature deviation as shown in Figure 10. Meaning that all channels will have similar outlet temperature regardless of the flow distribution. This is because of the large heat exchange area. When the heat conductivity of the wall material changes from 16 W/m.K for steel to 0.93 W/m.K for glass, the critical liquid residence time increases by two times. Reducing h_{mc} by half increases the critical residence time by 1.5 times. Moreover, when the microchannel diameter is reduced by half, the critical residence time decreases by more than 3 times.

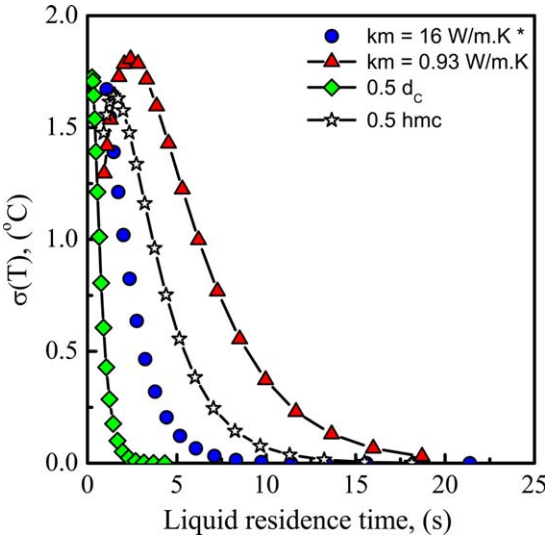

Figure 11. Effect of a 10% flow nonuniformity on temperature deviation at varied liquid residence time for the case shown in Figure 1010.

[Color figure can be viewed in the online issue, which is available at wileyonlinelibrary.com.]

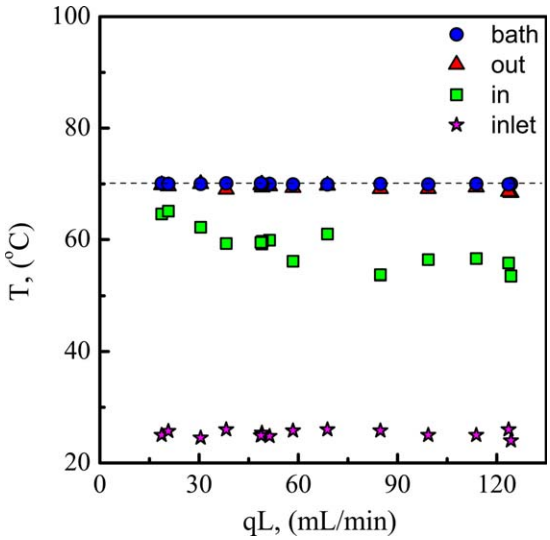

Figure 12. Steady-state temperature deviation at different flow rates.

Four liquid temperatures are measured: water bath T_{bath}, outlet from the gas-liquid microchannels T_{out}, inlet to the gas-liquid microchannels T_{in}, and inlet to the manifold T_{inlet}. [Color figure can be viewed in the online issue, which is available at wileyonlinelibrary.com.]

For a specific target flow nonuniformity, 10% was used here as an example, Figure 10 can be replotted as shown in Figure 11. For the entire tested flow distribution, temperature deviation $\sigma(T)$ remained less than 2°C. The flow rate effect on temperature deviation was not that significant. However, one should keep in mind that this study was made with uniform heat supply and without any reaction involved. Testing the effect of these factors on the temperature and flow distributions is an essential study to be explored in the future.

Experimental studies: Effect of temperature and flow distributions

The effect of liquid flow rate on temperature deviation is shown in Figure 12. The gas flow rate has no effect on the obtained result. The investigations were made at steady-state situation. Liquid temperatures were measured at four different locations as given in Figure 12, inlet to the manifold, T_{inlet}, inlet to the gas-liquid microchannels, T_{in}, outlet of the gas-liquid microchannels, T_{out}, and water heating bath, T_{bath}. It is good to remind here that only the gas-liquid microchannels were in contact with the water heating bath while the other BMMR parts (inlets, manifolds, barrier channels, and collector) were outside the water heating bath.

The temperature of the liquid inlet to the microchannels T_{in} is much larger than T_{inlet}. It reaches more than 60°C for some flow rates. The increase of T_{in} even before it enters the microchannels is due to the heat conduction. That is why T_{in} decreases as the flow rate increases. For the entire tested liquid flow rates, the temperature at the outlet of the gas-liquid

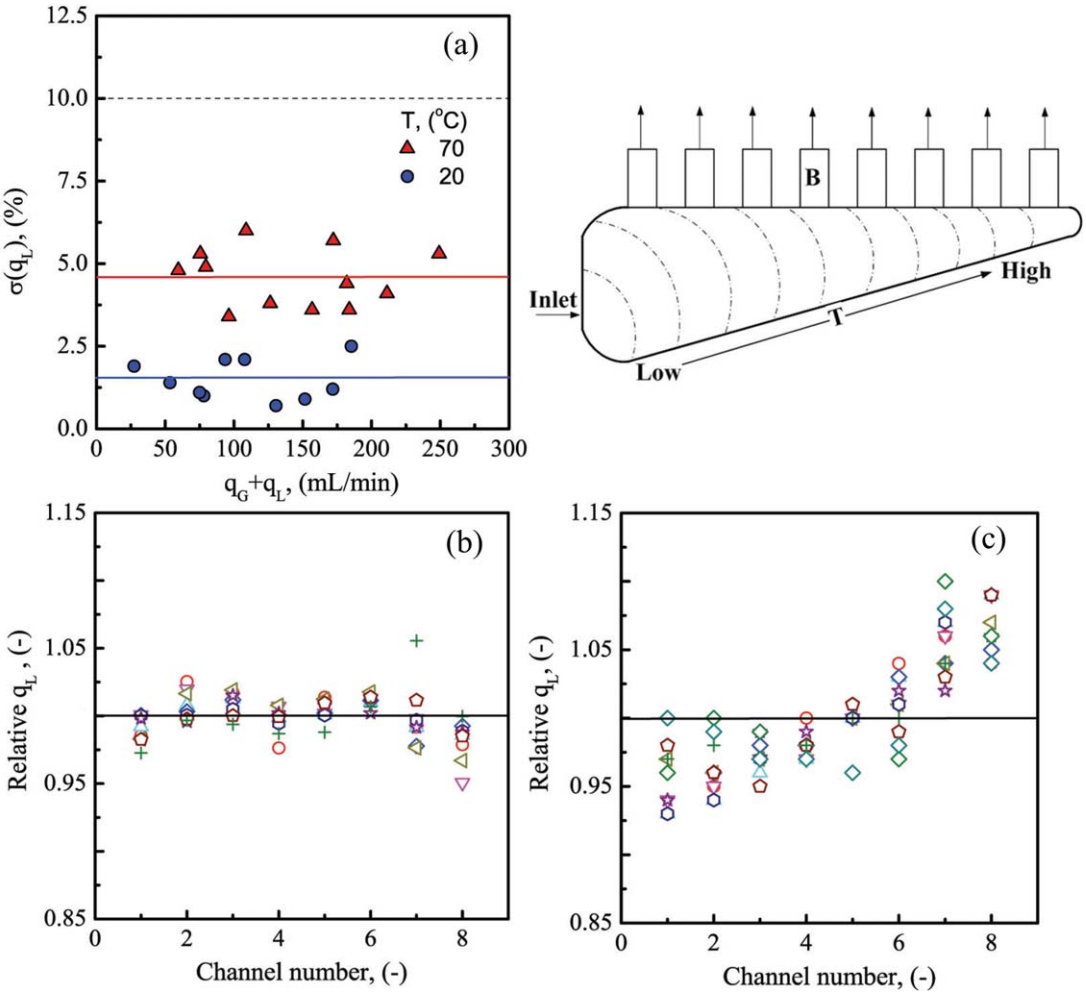

Figure 13. (a) Liquid flow nonuniformity at varied gas (from 10 to 230 mLn/min) and liquid (10–115 mL/min) flow rates at two temperatures at 20°C and 70°C; (b) and (c) are the relative flow rate per channel for all flow rates at 20°C and 70°C, respectively.

The schematic drawing show a top view of the liquid manifold, the inlet feed location, and the direction of increasing temperature in the manifold from Low to High. [Color figure can be viewed in the online issue, which is available at wileyonlinelibrary.com.]

microchannels T_{out} always reached the water bath temperature. The difference of T_{out} over the eight parallel microchannels remained always less than 1°C. This is due to the very large heat-transfer area of the BMMR. Thus, the liquid residence time in the BMMR was always larger than the critical liquid residence time.

The effect of temperature on flow distribution is shown in Figure 13a. The liquid flow nonuniformity remained less than 10% for the entire range of tested flow rates. Changing gas to liquid flow ratio at a constant liquid flow rate had no significant effect on flow distribution.

When the temperature increased from 20 to 70°C, flow nonuniformity increased by a factor of two. The increase in flow nonuniformity at 70°C is due to the temperature deviation in the barrier channels. The relative flow rate per channel is plotted as shown in Figures 13b and 13c. When the experiments were conducted at 70°C, the profile of flow distribution changes. Flow rate was the smallest near to the manifold inlet for microchannel number 1 and largest at the end of manifold for microchannel number 8. Figure 13 shows a top view of the liquid manifold with the position of manifold inlet and outlet to the barrier channels. The manifold was not in contact with the water heating bath, but gets heated due to the heat conduction via the metal connections. The temperature near the manifold inlet was the lowest (Low) while that in the last channel, microchannel 8, was the highest (High). When temperature increased, liquid viscosity decreased allowing larger flow rate in that specific channel to maintain similar pressure drop as those of the parallel microchannels. The profile of flow distribution took the shape of an inclined line; low near the manifold inlet and high near the last microchannel. This result demonstrates clearly the effect of temperature deviation in the barrier channels on flow distribution.

Conclusions

In this article, the effect of temperature on flow distribution was demonstrated for the BMMR. The 2-PRN model was used to compute the flow distribution for a predefined temperature deviation in three parts of the BMMR: manifolds, barrier channels, and mixer and reaction channels. Temperature deviation in the barrier channels has the strongest effect on flow distribution. Temperature deviation in the manifold has negligible effect on flow distribution. For a similar value of temperature deviation, the barrier channels

affect flow distribution 10 times more than the mixer and reaction channels. This value can change depending on the relation between the viscosity and temperature.

The 2-PRN model could not be used to study the effect of flow rate on temperature deviation. Instead, a one-dimensional energy balance was developed. Above a certain critical liquid residence time, flow rate had no significant effect on the temperature deviation. The critical liquid residence time depends on the liquid used, the BMMR material of construction and its geometrical dimensions.

A design methodology was proposed to provide cut-off values of the maximum allowed temperature deviation in the barrier channels and in the mixer and reaction channels. By combining this design methodology with the previously developed one on the effect of microchannel diameters, a complete engineering methodology was achieved for maintaining flow nonuniformity below a defined target. An example of how to keep flow nonuniformity lower than 10% was demonstrated.

Outlook

To operate the barrier-based distributor using another flow regime, the design methodology can still be used if a pressure drop correlation for the two-phase flow and how it is influenced is known. The scaling parameters for the design methodology are all given in term of pressure drops. That is why it is possible to use the design methodology for another flow regime. Verifying that experimentally still needs to be made.

The operating flow rate for the distributor is presented previously by the authors.[25] The operating flow rate of the design methodology is the same as that of the barrier-based distributor. However, it is important to note that the hydraulic RN used in this design methodology is only valid for relatively low *Re* numbers in the laminar regime. For larger *Re* numbers, the hydraulic flow resistances due to flow turning, contraction, expansion, and mixing, what is called singularity losses, can not be neglected and strongly influence the manifold performance. This is an issue of flow distribution for single-phase flow which can be approached separately. For the effect of variation in the hydraulic resistances in the barrier channels due to the variation in channels diameters and temperature deviation, no changes are anticipated on flow distribution at larger *Re* numbers. However, for the influence in the mixer and reaction channels, a case study using a detailed fluid mechanics analysis (numerical and/or experimental) can only bring clear answers to this question.

This study was performed with large degree of simplification. Nonetheless, it provided a quick estimation of the critical design parameters needed for the numbering-up like the diameter variations and temperature deviations. What is a real challenge next, is to design a heat exchanger which ensures a uniform heat supply or removal from the reaction microchannels. The second challenge is to test this design methodology in a real case which involves a reaction in the gas-liquid microchannels. Thus, exploring the relation between flow nonuniformities, temperature deviations, and their effect on the reaction conversion and selectivity.

Literature Cited

1. Kockmann N, Roberge DM. Harsh reaction conditions in continuous-flow microreactors for pharmaceutical production. *Chem Eng Technol*. 2009;32:1682–1694.
2. Charpentier JC. In the frame of globalization and sustainability, process intensification, a path to the future of chemical and process engineering (molecules into money). *Chem Eng J*. 2007;134:84–92.
3. Wiles C, Watts P. Continuous flow reactors: a perspective. *Green Chem*. 2012;14:38–54.
4. Hessel V, Cortese B, de Croon MHJM. Novel process windows—concept, proposition and evaluation methodology, and intensified superheated processing. *Chem Eng Sci*. 2011;66:1426–1448.
5. Anxionnaz Z, Cabassud M, Gourdon C, Tochon P. Heat exchanger/reactors (HEX reactors): concepts, technologies: state-of-the-art. *Chem Eng Process Process Intensification*. 2008;47:2029–2050.
6. Al-Rawashdeh M, Yu F, Nijhuis TA, Rebrov EV, Hessel V, Schouten JC. Numbered-up gas-liquid micro/milli channels reactor with modular flow distributor. *Chem Eng J*. 2012;207–208:645–655.
7. Kockmann N, Gottsponer M, Roberge DM. Scale-up concept of single-channel microreactors from process development to industrial production. *Chem Eng J*. 2011;167:718–726.
8. Hornung CH, Mackley MR, Baxendale IR, Ley SV. A microcapillary flow disc reactor for organic synthesis. *Org Process Res Dev*. 2007:11:399–405.
9. Hessel V, Knobloch C, Loewe H. Review on patents in microreactor and micro process engineering. *Recent Patents Chem Eng*. 2008;1:1–16.
10. Lerou JJ, Tonkovich AL, Silva L, Perry S, McDaniel J. Microchannel reactor architecture enables greener processes. *Chem Eng Sci*. 2010;65:380–385.
11. Schenk R, Hessel V, Hofmann C, Loewe H, Schoenfeld F. Novel liquid-flow splitting unit specifically made for numbering-up of liquid/liquid chemical microprocessing. *Chem Eng Technol*. 2003;26:1271–1280.
12. Roberge DM, GOttsponer M, Eyholzer M, Kockmann N. Industrial design, scale-up, and use of microreactors. *Chem Today*. 2009:27:8–11.
13. Saber M, Commenge JM, Falk L. Heat-transfer characteristics in multi-scale flow networks with parallel channels. *Chem Eng Process Process Intensification*. 2009:49:732–739.
14. Kashid MN, Gupta A, Renken A, Kiwi-Minsker L. Numbering-up and mass transfer studies of liquid-liquid two-phase microstructured reactors. *Chem Eng J*. 2010;158;233–240.
15. Mendorf M, Nachtrodt H, Mescher A, Ghaini A, Agar DW. Design and control techniques for the numbering-up of capillary microreactors with uniform multiphase flow distribution. *Ind Eng Chem Res*. 2010;49:10908–10916.
16. Yue J, Boichot R, Luo L, Gonthier Y, Chen G, Yuan Q. Flow distribution and mass transfer in a parallel microchannel contactor integrated with constructal distributors. *AIChE J*. 2010;56:298–317.
17. Natividad R, Cruz-Olivares J, Fishwick RP, Wood J, Winterbottom JM. Scaling-out selective hydrogenation reactions: from single capillary reactor to monolith. *Fuel*. 2007;86:1304–1312.
18. Chambers RD, Fox MA, Holling D, Nakano T, Okazoe T, Sandford G. Elemental fluorinePart 16. Versatile thin-film gas-liquid multi-channel microreactors for effective scale-out. *Lab Chip*. 2005;5:191–198.
19. Amador C, Gavriilidis A, Angeli P. Flow distribution in different microreactor scale-out geometries and the effect of manufacturing tolerances and channel blockage. *Chem Eng J*. 2004;101:379–390.
20. Commenge JM, Falk L, Corriou JP, Matlosz M. Optimal design for flow uniformity in microchannel reactors. *AIChE J*. 2002;48:345–358.
21. Mason BP, Price KE, Steinbacher JL, Bogdan AR, McQuade DT. Greener approaches to organic synthesis using microreactor technology. *Chem Rev*. 2007;107:2300–2318.
22. Rebrov EV, Schouten JC, de Croon MHJM. Single-phase fluid flow distribution and heat transfer in microstructured reactors. *Chem Eng Sci*. 2011;66:1374–1393.
23. Wada Y, Schmidt MA, Jensen KF. Flow distribution and ozonolysis in gas-liquid multichannel microreactors. *Ind Eng Chem Res*. 2006;45:8036–8042.
24. De Mas N, Gunther A, Kraus T, Schmidt MA, Jensen KF. Scaled-out multilayer gas-liquid microreactor with integrated velocimetry sensors. *Ind Eng Chem Res*. 2005;44:8997–9013.
25. Al-Rawashdeh M, Fluitsma LJM, Nijhuis TA, Rebrov EV, Hessel V, Schouten JC. Design criteria for a barrier-based gas-liquid flow distributor for parallel microchannels. *Chem Eng J*. 2012;181–182:549–556.
26. Al-Rawashdeh M, Nijhuis TA, Rebrov EV, Hessel V, Schouten JC. Design methodology for barrier-based two phase flow distributor. *AIChE J*. 2012;58-11:3482–3493.

27. Leung SS, Gupta R, Fletcher DF, Haynes BS. Effect of flow characteristics on Taylor flow heat transfer. *Ind Eng Chem Res*. 2012;51: 2010–2020.
28. Haber J, Kashid MN, Renken A, Kiwi-Minsker L. Heat management in single and multi-injection microstructured reactors: Scaling effects, stability analysis, and role of mixing. *Ind Eng Chem Res*. 2012;51:1474–1489.
29. Goletz E, Tassios D. An antoine type equation for liquid viscosity dependency to temperature. *Ind Eng Chem Process Des Dev*. 1977;16:75–79.
30. Chung TH, Ajlan M, Lee LL, Starling KE. Generalized multiparameter correlation for nonpolar and polar fluid transport properties. *Ind Eng Chem Res*. 1988;27:671–679.

Manuscript received Feb. 13, 2013, and revision received June 24, 2013.